



# Programming of drug release via rolling-up of patterned biopolymer films

Riccardo Pedron, Thierry Vandamme, Valeriy Luchnikov

## ► To cite this version:

Riccardo Pedron, Thierry Vandamme, Valeriy Luchnikov. Programming of drug release via rolling-up of patterned biopolymer films. *Nano Select*, 2021, 2 (5), pp.948-957. 10.1002/nano.202000126 . hal-03431737

HAL Id: hal-03431737

<https://hal.science/hal-03431737>

Submitted on 23 Nov 2021

**HAL** is a multi-disciplinary open access archive for the deposit and dissemination of scientific research documents, whether they are published or not. The documents may come from teaching and research institutions in France or abroad, or from public or private research centers.

L'archive ouverte pluridisciplinaire **HAL**, est destinée au dépôt et à la diffusion de documents scientifiques de niveau recherche, publiés ou non, émanant des établissements d'enseignement et de recherche français ou étrangers, des laboratoires publics ou privés.

# Programming of drug release via rolling-up of patterned biopolymer films

Riccardo Pedron<sup>1</sup> | Thierry Vandamme<sup>1</sup> | Valeriy A. Luchnikov<sup>2</sup> 

<sup>1</sup> Faculty of Pharmacy, University of Strasbourg, CNRS UMR 7199, Laboratoire de Conception et Application de Molécules Bioactives (CAMB), équipe de Pharmacie Biogalénique, Illkirch Cedex, France

<sup>2</sup> Université de Haute-Alsace, CNRS, IS2M UMR 7361, Mulhouse, France

## Correspondence

Valeriy A. Luchnikov, Université de Haute-Alsace, CNRS, IS2M UMR 7361, 15, Rue Jean Starcky, F-68100 Mulhouse, France.  
Email: [valeriy.luchnikov@uha.fr](mailto:valeriy.luchnikov@uha.fr)

## Abstract

Continuous progress of personalized medicine is insistently calling the pharmaceutical sector to increase product variability more than ever before. One of the challenges consists in personalization of the drug release rates and doses from drug-containing media. Herein is introduced an innovative methodology which resolves this problem by combining inkjet printing and rolling up procedure, allowing for the production of capsules with tailorabile distributions of medical compounds. The prototype capsules consist of rolled-up polymeric films over which fluorescent probes have been deposited via inkjet printing prior to rolling. The position of the probes inside the capsules are determined by the printed 2D pattern. The delay and the rate of the release of the probes in dissolution media can be shaped by the number of rolls and the position of the drug reservoir on the polymeric film before rolling. The innovative method proposed in the paper paves the way to a novel family of drug delivery devices with a broad range of therapeutic applications and it stands alongside other additive manufacturing techniques but allows to avoid their usual constraints.

## KEY WORDS

additive manufacturing, controlled release, personalized medicine, rolling up

## 1 | INTRODUCTION

Personalized medicine, a novel medical model that tailors the therapy on the patient needs,<sup>[1,2]</sup> is having a strong impact over all the health care system and novel drug entities are continuously being approved by the FDA,<sup>[3]</sup> but still many challenges need to be overcome before its general acceptance. The emergence of new individualized therapies indeed, requires a dramatic change over the pharmaceutical manufacturing and supply chain landscape,<sup>[4]</sup> which has historically relied on large volume production with limited variability. Nevertheless, the current manufacturing methodologies display a small window

for customization and the number of dose and type of formulations available on the market is limited.<sup>[5,6]</sup>

Adaptation of drug release kinetics to a patients' metabolism rate<sup>[7]</sup> and its individual circadian rhythm<sup>[8,9]</sup> are important parts of the drugs personalization strategy. Many pathologies, including hypertension, cancer, bronchial asthma, myocardial infarction can be more effectively treated by optimization of drug administration timing. By ensuring higher dosage flexibility, multi-dose formulations might be considered the most immediate and effective solution to the problem, but they usually suffer from poor dose accuracy and reduced shelf life which cannot be always accepted especially for drugs with high

This is an open access article under the terms of the Creative Commons Attribution License, which permits use, distribution and reproduction in any medium, provided the original work is properly cited.

© 2021 The Authors. *Nano Select* published by Wiley-VCH GmbH

potency and low therapeutic index.<sup>[10]</sup> Instead, flexible technologies such as additive manufacturing and inkjet printing are the most promising tools for personalized medicine production at industrial scale.<sup>[11,12]</sup> In fact, by enabling customizable and small batch production, they allow increasing product variety meanwhile keeping low inventory levels.<sup>[4]</sup>

With the first FDA approval of 2015,<sup>[13]</sup> additive manufacturing, also known as 3D printing, is for sure one of the front-line technology for patient-specific medicine with high-resolution control over dosage composition and customization of release profiles.<sup>[5,14]</sup> However, each of the 3D printing methodologies shows constraints which limit their real adaptability. Indeed, the stability of the active principle should be evaluated case by case, especially for techniques employing thermal or light-induced curing, furthermore removal of residual monomers, solvents or initiators must be considered.<sup>[15,16]</sup>

Even though inkjet printing is a rather new concept for the pharmaceutical industry,<sup>[17]</sup> it is a very well-established technology in other manufacturing sectors as a non-contact surface patterning technique.<sup>[18]</sup> Thanks to its deposition accuracy and precision, inkjet printing revealed itself as a valuable tool for the production of low-dose medicines<sup>[11]</sup> and promising results have been obtained to increase the water solubility of poorly soluble drugs.<sup>[19,20]</sup>

The intrinsic flexibility of inkjet printing paved the way for development in personalized dosing methodologies. Interesting are the works of Voura et al.<sup>[21]</sup> and Genina et al.<sup>[22]</sup> which independently introduce a similar method for preparation of dose-customizable dosage forms via a continuous manufacturing process.

In the present paper, we propose further development of personalized low-dose medicines characterized by controllable and programmable release kinetics by combining the ink-jetting technique with the rolling-up microfabrication approach. Rolling-up is a powerful yet simple method for creation of objects with complex internal structure, which find numerous applications in such different fields as microfluidics,<sup>[23]</sup> optics,<sup>[24]</sup> and many others.<sup>[25,26]</sup> It is not surprising that it can be useful for the design of medicines with tailororable characteristics. The first steps in this direction were made a half of century ago by Higuchi, who has invented a “swiss-roll” tablet,<sup>[27]</sup> which was designed to release the drugs in course of erosion of the matrix. Yet, his system did not find broad application, probably because erosion is generally a poor controllable process. The system proposed in the present paper is based on the diffusion and dissolution-controlled release from a drug reservoir, embedded in a biopolymer membrane. The rate and the lag time of the release are determined by the drug distribution on the polymer stripe before rolling.

Apart of the experimental study, we have undertaken computer simulation of the drug release from the reservoirs embedded in between the layers of a rolled-up capsule. The model is particularly useful for prediction of non-trivial kinetics, which can be realized by combining several drug reservoirs, characterized by their individual surface, amount of loaded drug, and the position with respect to the capsule’s surface. In particular, it is shown that the proper choice of the parameters of the reservoirs can result in the kinetics with two quasi-zero-order release phases. More complex kinetics, including the multidrug ones, seem to be also realizable in frames of the approach.

## 2 | MATERIALS AND METHODS

### 2.1 | Fabrication of capsules

The proposed system is a cylinder formed by rolling up a chitosan acetate (CA) film, over which has been printed fluorescein disodium (FD) pattern. FD (Figure S1a of the S.I.) was chosen as the model drug due to its detectability at very low concentrations in water solutions. The CA (Figure S1b of the S.I.) film was prepared by casting solution of low molecular weight chitosan in glacial acetic acid with the use of a film casting knife and drying in controlled conditions. Its average thickness in dry state was estimated as  $h_0 \approx 42\mu\text{m}$ . The homogeneity of the film was measured with a micrometric screw and the standard deviation was found to be in the limit of 11% of the mean value. The model drug pattern was printed over the polymeric film with a drop-on-demand inkjet Dimatix materials printer. In order to provide good adhesion of the ink to the CA films, polyethylene glycol (PEG) was added to the ink formulation (see the Section S1 of the Supporting Information [SI] for more details). The film was rolled over a polycaprolactone (PCL) stick, prepared by extrusion. The number of the layers in the roll varied from  $n_{turns} = 2$  to  $n_{turns} = 11$ . The radius of the stick,  $R = 2.3\text{mm}$ , was essentially greater than the largest thickness of the multilayer membrane in the swollen state,  $h = 11h_0\alpha \approx 0.73\text{mm}$ , where  $\alpha \approx 1.58$  is the swelling factor of the films in the phosphate buffer solution, served the release media. This value has been obtained by the square root of the area swelling ratio (see the Section S1 of the Supporting Information [SI] for more details) (Figure 1).

The film can be virtually divided on zones corresponding to each turn of the film around the PCL stick. The winded film is best described by the Archimedean spiral,  $r(\varphi) = R + \frac{h_0}{2\pi}\varphi$ . Since  $R \gg h_0$ , the winded membrane can be approximated by set of concentric cylindrical shells. The perimeters of the shells follow the

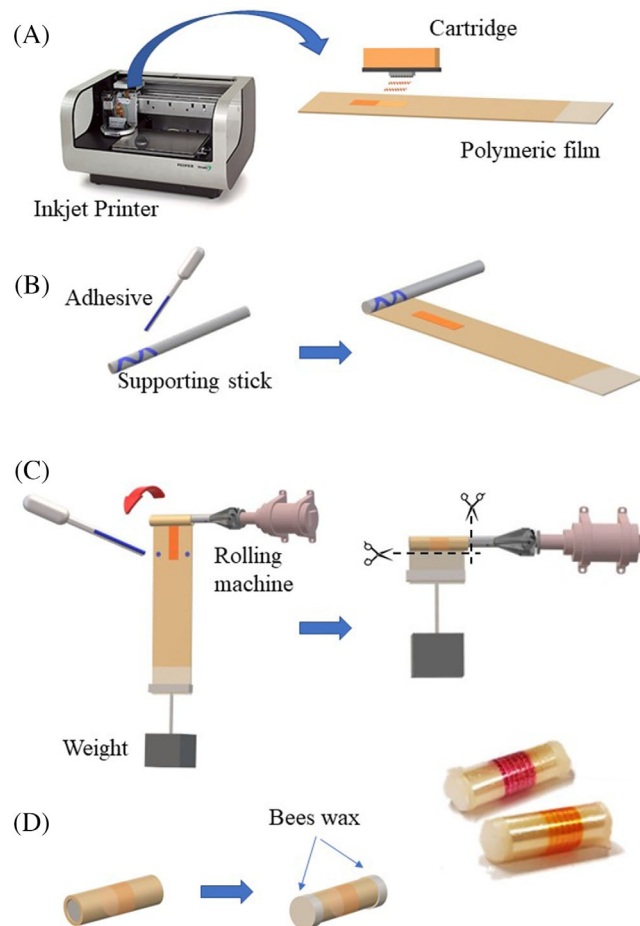


**FIGURE 1** Roll's fabrication procedure. A, The model drug is printed over the polymeric film with the inkjet printer, then (B) a supporting stick have been attached over its extremity corresponding to the inner turn of the roll. C, During the rolling two drops of the water-resistant adhesive are placed at the two extremities of the film at each turn, then the excess of film and supporting stick are cut away. D, the axial extremities of the roll are coated with beeswax. At the right bottom side, the picture of two rolls is reported, the red one with rhodamine B chloride printed at the 10<sup>th</sup> turn the orange one with disodium fluorescein printed at the 10<sup>th</sup> turn

arithmetic progression  $l_n = 2\pi R + 2(n - 1)\pi h_0$ , which determine the length of the zones on the stripe, corresponding to the shells (see Figure S2 of the SI). The coordinates of the limits of the  $n$ th zone are calculated as the respective sums of the progression,  $s_{n-1} = 2\pi(n - 1)R + \pi(n^2 - 3n + 2)h_0$ ,  $s_n = 2\pi n R + \pi(n^2 - n)h_0$ , that is,  $[s_{n-1}, s_n] = [0, 2\pi R], [2\pi R, 4\pi R + 2\pi h_0], \dots$ . In the following, we use the nomenclature  $p/n_{turns}$  to designate a roll, which consists of  $n_{turns}$ , and has the printed pattern on the  $p^{th}$  shell. For instance, 4/11 will mean the roll, which consists of 11 total turns, and contain the reservoir at the 4<sup>th</sup> shell. The films are rolled so that the printed pattern is on the concave side of the shell. Therefore, in the aforementioned example of the 4/11 roll, the distance

from the ink reservoir to the PCL core is  $a = (p - 1) \alpha h_0 \approx 200 \mu m$ ; the distance from the reservoir to the surface is  $h = a = n^* \alpha h_0 \approx 530 \mu m$ , where  $n^* = (n_{turns} - [p - 1])$  is the number of the barrier layers between the reservoir and the surface of the capsule. The film rolling is performed with the help of a rolling machine built for the scope. It consists of an engine at which shaft has been attached a drill's chuck. Prior to rolling, the CA film was attached to the PCL stick by water-resistive adhesive (Eudragit RS PO). To perform the rolling, one extremity of the stick is inserted inside the chuck by letting the film fall vertically. To keep the film under constant tension during the rolling, a weight was connected with a clamp at the falling extremity of the film. The length of the polymeric film was calculated to have a precise number of turns over the supporting stick, plus an excess of one cm in length reserved for this weight's clamp. During the rolling, at the end of each turn, two drops of the water-resistant adhesive were deposited at the two sides of the film. Once the rolling was finished the excess of polymeric film and supporting stick was cut away. Finally, the axial extremities of the obtained cylinder were coated with beeswax to prevent water penetration from the extremities during the dissolution assay.

The average approximate characteristics of the ink, the CA film and the ink reservoir are summarized in the Table 1.

## 2.2 | Fluorescein release study

Dissolution study were performed with Flow through cell closed loop offline system purchased by Erweka. There were used 22,6 mm tablet cells with one glass ball. Flow was kept at 8 mL/min.

The dissolution media was phosphate buffer 0,2 M, pH = 7,40 at 37°C. For F first release study in which was changed the total number of turns of the roll, 1020 mL of dissolution media were used, meanwhile 250 mL for multi model drug release 250 mL.

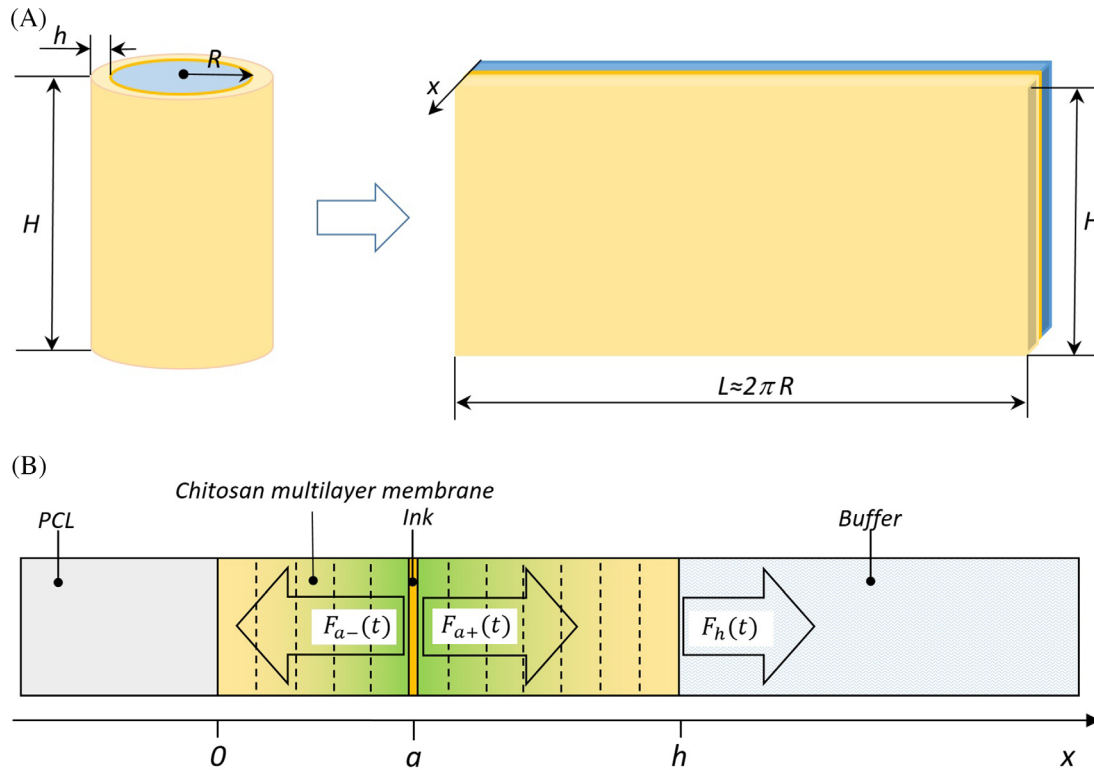
Quantification of fluorescein concentration were done in phosphate buffer 0,2 M pH = 7,40 by fluorescence with the microplate reader Varioskan LUX in (Ex/Em: 490 nm/520 nm for fluorescein with Thermo Scientific NUNC 96 well black plates for fluorescence measurements.

## 2.3 | Computer simulation model

The possibilities of the rolling-up approach for the kinetics programming was explored via computer simulation, based on the standard theoretical methods.<sup>[28,29]</sup> Since the radius of the supporting PCL stick is about three times

**TABLE 1** Parameters of the film and the ink reservoir

$C_0, \mu\text{g} \cdot \text{cm}^{-3}$	$h_0, \mu\text{m}$	$S, \text{cm}^2$	$M_{ink}, \mu\text{g}$
$7.01 \cdot 10^5$	42	0.75	640

**FIGURE 2** To the computer simulation of the model drug release. A, Transformation of a cylindrical drug release system into the equivalent rectangular system. B, Structure of the release system in the direction normal to the membrane

larger than the maximal thickness of the multilayer rolled-up membrane, the cylindrical drug-release system was replaced by equivalent rectangular system (Figure 2A). This approximation, which seems to be justified at the present level of accuracy of the release kinetics measurements, allows to simplify greatly the model by passing from the cylindrical coordinates to the cartesian ones. It is assumed also, that the diffusion and the partition coefficients (and  $K$ , respectively) do not depend on the ink concentration. Under these assumptions, it is possible to obtain the analytical solutions for the kinetics in form of Fourier series.

The structure of the release system is shown schematically by the Figure 2B. A infinitely thin reservoir is embedded between two layers of the membrane at the distance  $x = a$ , and contains  $M_{ink}$  micrograms of the model drug. The drug reservoir is considered as constant concentration source, that is, the concentration in the membrane at the source is sustained at the constant level  $KC_0$  ( $K$  is the partition coefficient, and  $C_0$  is the saturation concentration of

FD in the buffer) until the drug is completely dissolved. The surface of the membrane, opposite to the PCL core and adjacent to the buffer solution, is supposed to be the perfect sink, since the concentration of the drug in the buffer is sustained at small level compared to the FD concentration in the membrane. We also suppose the membrane to be monolithic, that is, assume that ink diffuses as if there is no interfaces between the layers.

Concisely, the algorithm of solution for the release profiles is the following one. Suppose that  $\tau$  is the time at which all drug is dissolved and evacuated from the reservoir. For  $t \leq \tau$  one should solve separately the diffusion equation on the concentration  $C_{0a}(x, t)$ , defined on the interval  $x \in [0, a]$ , and on the concentration  $C_{ah}(x, t)$ , defined on the interval  $x \in [a, h]$ . The boundary conditions (B.C.) for  $t \leq \tau$  read

$$\left. \frac{\partial C_{0a}}{\partial x} \right|_{x=0} = 0, \quad C_{0a}(a, t) = KC_0 \quad (1)$$

$$C_{ah}(a, t) = KC_0, \quad C_{ah}(h, t) = 0 \quad (2)$$

The B.C. (1) have the physical meaning of the absence of flux through the membrane/PCL interface, and the constant concentration at the model drug reservoir. The B.C. (2) signify the constant concentration at the drug source, and the perfect sink at the membrane/buffer interface.

The initial conditions (I.C.) read for the two intervals:

$$C_{0a}(x, 0) = 0 \text{ for } x \in [0, a[ ; C_{ah}(x, 0) = 0 \text{ for } x \in ]a, h] \quad (3)$$

The drug is evacuated from the reservoir by the flux  $F_{a-}(t) = SD \frac{\partial C_{0a}}{\partial x} |_{x=a}$  in the direction of the PCL core, and by the flux  $F_{a+} = -SD \frac{\partial C_{ah}}{\partial x} |_{x=a}$  in the direction of the capsule's surface. The moment  $\tau$  is determined by the numerical solution of the equation

$$\int_0^\tau F_{a-}(t) dt + \int_0^\tau F_{a+}(t) dt = M_{ink} \quad (4)$$

For  $t \geq \tau$ , the diffusion equation for the concentration  $C(x, t)$  is solved on the interval  $[0, h]$  with the B.C.

$$\left. \frac{\partial C}{\partial x} \right|_{x=0} = 0, \quad C(h, t) = 0 \quad (5)$$

and the I.C.

$$C(x, \tau) = \begin{cases} C_{0a}(x, \tau), & x \in [0, a] \\ C_{ah}(x, \tau), & x \in [a, h] \end{cases} \quad (6)$$

The flux from the surface of the membrane into the buffer is

$$F_h(t) = \begin{cases} -SD \frac{\partial C_{ah}}{\partial x} |_{x=h}, & t \leq \tau \\ -SD \frac{\partial C}{\partial x} |_{x=h}, & t \geq \tau \end{cases} \quad (7)$$

The released amount is, respectively,

$$M(t) = \int_0^h F_h(t) dt = \begin{cases} -SD \int_0^t \frac{\partial C_{ah}(x, \tilde{t})}{\partial x} \Big|_{x=h} d\tilde{t}, & t \leq \tau \\ -SD \int_0^\tau \frac{\partial C_{ah}(x, t)}{\partial x} \Big|_{x=h} dt - SD \int_\tau^h \frac{\partial C(x, \tilde{t})}{\partial x} \Big|_{x=h} d\tilde{t}, & t \geq \tau \end{cases} \quad (8)$$

The explicit expressions for (5) - (7) are rather bulky (although their calculation is straightforward); for this reason, they are given in the S.I., Section S2.

The above formulas assume that the dissolution in the drug reservoir starts at  $t = 0$ . In reality, one should take into account the lag time  $\theta$ , which is due to non-

instantaneous penetration of the buffer from the surface of the membrane to the position of the reservoir, and possibly due to competition of PEG and FD for water, discussed below.

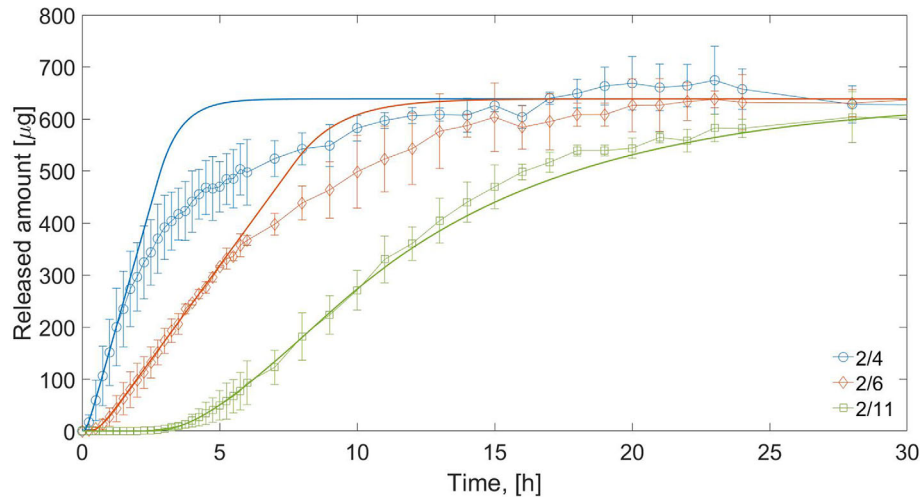
The fitting procedure of the experimental kinetics by the model ones is described in the S.I., Section S3.

### 3 | RESULTS AND DISCUSSION

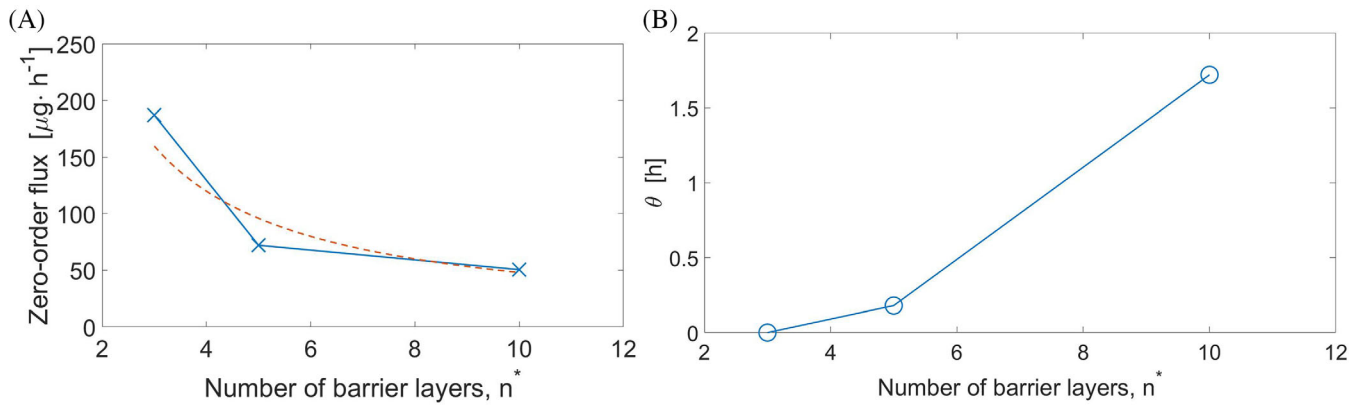
#### 3.1 | Kinetics for the drug reservoir at the PCL core and increasing number of CA layers

Figure 3 shows the experimental kinetics of FD release from the capsules with the drug reservoir placed at the second turn of the film, for the increasing total number of the turns  $n_{turns}$  running from 4 to 11. The solid lines on the same figure show the fitting of the experimental curves by computer simulation, according the procedure described in the Section S3 of S.I. It is possible to identify on the experimental kinetics the intervals of quasi-linear grow of the released amount of drug (zero-order release). The release rate during this phase,  $F_{z.o.}$ , determined by the means squares method, is shown by the solid line on the Figure 4A as the function of the number of layers, separating the reservoir from the surface of the capsule (number of barrier layers,  $n^*$ , defined above). From the formula  $F_{z.o.} = \frac{KDC_0S}{h-a} = \frac{KDC_0S}{n^*h_0^\alpha}$  (the constant part of Eq.(50), S.I.) and the known parameters  $C_0$ ,  $S$ ,  $h$  and  $a$  one can deduce the effective transport coefficient of the multilayer membrane,  $P = KD$ . Also, one should take into account, that as in the case of other film-coated devices,<sup>[29,30]</sup> a lag time is expected before the beginning of the release of the fluorescent probe after having placed the roll in the dissolution medium.

Using the expression (33) of the S.I. for the released amount of drug before and during the zero-order phase, and applying the lag time  $\theta$  as the fitting parameter, we have made an attempt to recover the coefficients  $K$  and  $D$  for the set of the kinetics presented on the Figure 3. The obtained values of  $K$ ,  $D$  and  $KD$  (see Table 2) which are supposed to be independent on the number of layers in the membrane have the dispersion within 30% of the respective average values. However, this result should be taken with caution, first because of significant statistical dispersion of the released amount, but also because the model gives only a simplified picture of the early and the final stages of the model drug release. Indeed, the lag times obtained by fitting the experimental curves with the computer simulation model seem to be well superior to the time necessary for the buffer to swell the membrane. An auxiliary experiment, in which a pH indicator,



**FIGURE 3** Release kinetics for the 2/X rolled-up capsules (dash lines, markers), and their fitting by the model (solid lines)



**FIGURE 4** A, Zero-order release rate as function of the number of layers between the drug reservoir and the membrane/buffer interface. Dashed line: fitting by the formula  $F_{z.o.} = \frac{\langle KD \rangle C_0 S}{h_0 \alpha n^*}$ , where  $\langle KD \rangle$  is the mean value of the membrane transport coefficient, see Table II. B, Lag time  $\theta$ , determined by the fitting procedure described in the Section S2.4, S.I

bromocresol purple, was placed on the 2nd turn of 11 turns roll (see Section S4, S.I.) suggests that buffer penetrates to the indicator reservoir within the first 15 minutes of the contact with the solvent. The additional lag time might be attributed to a delay of the fluorescein dissolution inside the reservoir. The PEG contained in the depot along with fluorescein can compete with this dye for water. Fluores-

cein inside the depot seem to be dissolved in a PEG amorphous matrix, as observed by SEM images (Figure S13, S.I.). Therefore, to diffuse out the roll, the PEG depot must swell, allowing the release of fluorescein. The PEG swelling is consequently proportional to the rate of water penetration inside the system, which decreases with the increasing number of turns.

**TABLE 2** Parameters of the kinetics, found by fitting the experimental data

	2/4	2/6	2/11	< >	$\sigma$
$F_{z.o.} [\mu\text{g} \cdot \text{h}^{-1}]$	187	73	50		
$D [\text{cm}^2 \cdot \text{s}^{-1}]$	$0.99 \cdot 10^{-7}$	$1.10 \cdot 10^{-7}$	$0.73 \cdot 10^{-7}$	$0.94 \cdot 10^{-7}$	$0.19 \cdot 10^{-7}$
K	0.020	0.012	0.024	0.019	0.006
$KD [\text{cm}^2 \cdot \text{s}^{-1}]$	$1.98 \cdot 10^{-9}$	$1.32 \cdot 10^{-9}$	$1.75 \cdot 10^{-9}$	$1.68 \cdot 10^{-9}$	$0.34 \cdot 10^{-9}$
$\theta [\text{h}]$	0	0.18	1.72		

The zero-order release rate,  $F_{z.o.}$ , fitted diffusion coefficient,  $D$ , partition coefficient,  $K$ , transport coefficient,  $P = KD$ , and lag time,  $\theta$ , for 2/X capsules.

The simulated kinetics 2/4 and 2/6 deviate strongly from the corresponding experimental kinetics on the last stage of release. The deviation may come also from the approximation of the roll's consecutive membranes as a unique slab, meanwhile each one is separated from the other, due to deformation of the swollen layers. Consequently, the volume of the roll is underestimated, and it can accumulate more dissolved drug than assumed by the model. This means that the drug in the reservoir is dissolved earlier than expected. Respectively, the concentration profile starts to decay to zero earlier than predicted by the model. With the increasing of the thickness of the membrane, the discrepancy of the simulated and the experimental kinetics at the late stages of the release is less evident, probably because the termination of the drug in the reservoir has the retarded effect on the drug release from the surface of the capsule. Indeed, the flux from the membrane surface is determined by the derivative of the concentration profile at the membrane/buffer interface (see Eq. 7). Yet, the deformation of this profile happens after a certain time interval after the drop of the drug source activity (see Figure S4, S.I.). The discrepancy of the theoretical and the experimental curves seems to be then in the limits of the statistical error.

A more advanced model will take into account also interaction of the model drug and the matrix. Yet, the fact that the amount of the released FD corresponds approximately to the quantity of the printed FD, suggests that interaction of the model drug with the chitosan membrane is relatively low, and in this sense FD/chitosan form almost ideal pair for testing the approach. To explain the interaction between chitosan and fluorescein, it is necessary considering their chemical structures properties and the nature of the dissolution medium. Despite the cationic charges of the chitosan's ammonium groups might have electrostatic interactions with anionic dyes, several factors are preventing this interaction between chitosan and fluorescein. The pKa of chitosan is close to 6,5,<sup>[31]</sup> therefore at the pH of the dissolution medium (pH = 7,4) only a small fraction of the amino groups is protonated, and the chitosan's monomers are for the most neutral. Furthermore, the phosphate anions of the buffer (0,2M) and the hydroxylate anions compete with fluorescein for the residual chitosan's cationic sites, reducing, even more, the possibility of electrostatic interaction between chitosan and fluorescein. To conclude it is worth remembering that the steric hindrance of the phenyl-xanthene moiety can prevent the approach to the chitosan's cationic sites of the fluorescein carboxylate group, where there is the highest density of negative charge. Indeed, Pirillo et al., in an adsorption study of dyes over a series of adsorbants, demonstrated that chitosan in distilled water between pH 5 and pH 9 is not an effective adsorbant for fluorescein.<sup>[32]</sup> Chitosan is

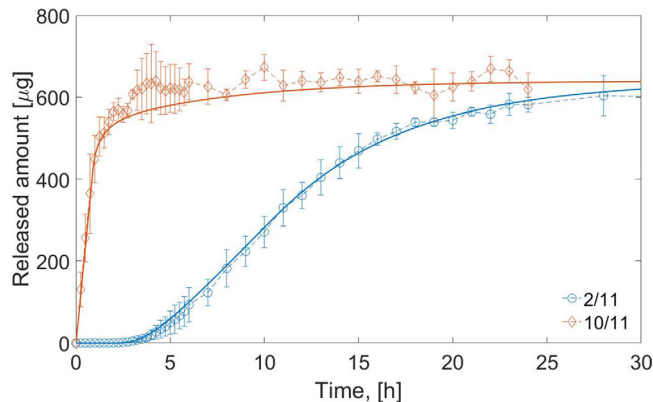


**FIGURE 5** Release kinetics for the 2/11 and 10/11 rolled-up capsules, and their fitting by the computer model

almost ideal choice for our study also thanks to its excellent film forming properties. It is a heteropolysaccharide composed of two randomly distributed monomers: glucosamine and N-acetylglucosamine. The most abundant is always glucosamine which is at the origin of the chitosan's basicity. Due to its amino groups chitosan is normally insoluble in neutral, basic solutions where it forms physical hydrogels. Instead, it is soluble in acidic solutions where it is in its polycationic state. Thin films that behave as physical hydrogel in our experimental conditions can be prepared by casting of chitosan dissolved in diluted acetic acid.

### 3.2 | Kinetics for a fixed number of CA layers and varied position of the drug reservoir

Instead of increasing the number of turns, one can program the release kinetics by placing the drug reservoir at different layers inside a membrane whose number of layers is fixed. To this end, the drug reservoir is printed on the corresponding zones of the stripes (see Figure S2, S.I.), which all have the same length. Technologically, such approach may be more convenient, since one can optimize the fabrication of capsules from the stripes of a fixed length, and just reprogram the printing of the drug reservoir. Figure 5 shows the release kinetics for the 2/11 capsules, and the 10/11 capsules, as well as their fitting by the computer model. The average values of  $D$  and  $K$  from the Table II are used for the simulation of the both kinetics. The respective lag times are  $\theta_{2/11} = 1.71\text{ h}$  (taken from the Table II) and  $\theta_{10/11} = 0$  (assumed).

In the case of such “position-programmed” release devices, one should take into account the influence of the drug diffusion from the reservoir in the direction opposite to the capsule surface (the retrodiffusion), which can

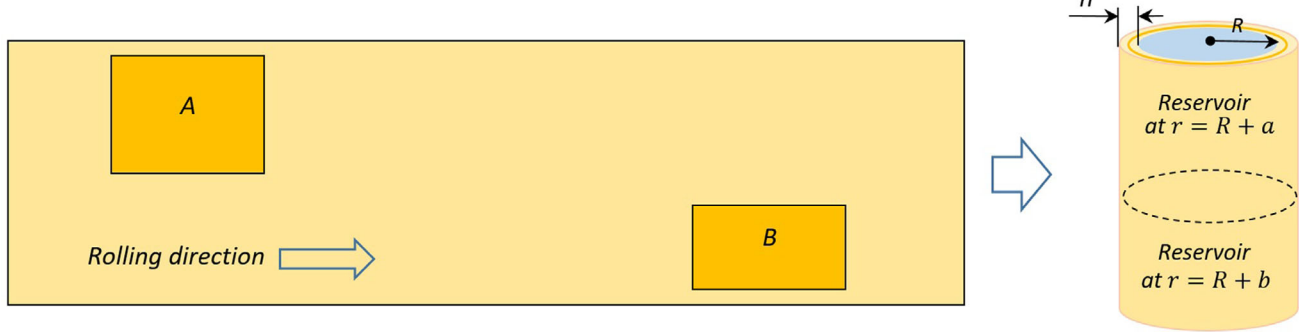


**FIGURE 6** Scheme of fabrication of a system with two embedded independent reservoirs

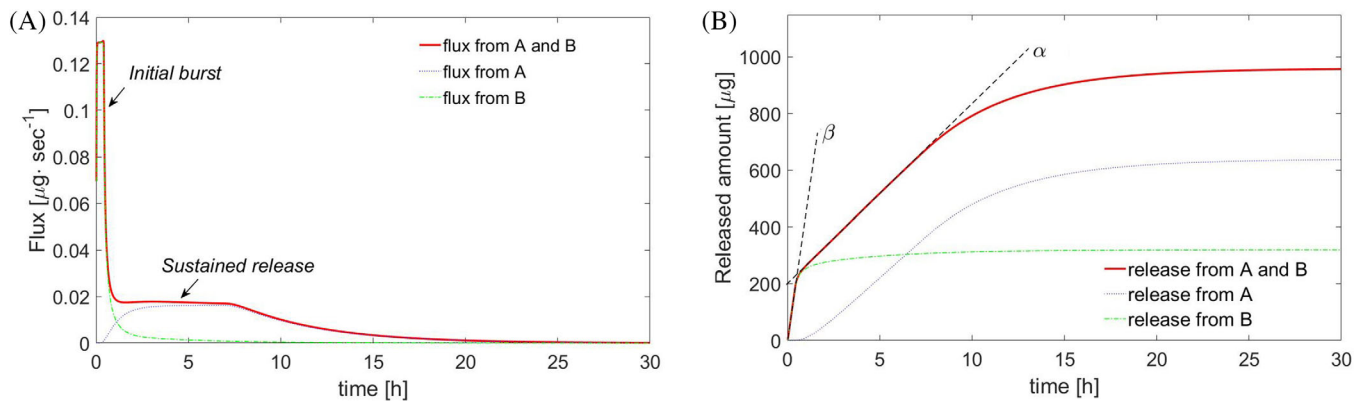


**FIGURE 7** Flux and release from a capsule with 2 reservoirs, *Simulation 1*. The kinetics has two distinct quasi-zero-order phases (marked by the dashed straight lines  $\alpha$  and  $\beta$ )

diminish the duration of the zero-order release phase, or even prevent it, if the amount of drug in the reservoir is not sufficiently large.

### 3.3 | Computer simulation of the kinetics for the capsules with 2 independent reservoirs

In this Section we consider, by means of the computer simulation, the case of a capsule which contains two drug reservoirs,  $A$  and  $B$ , characterized by respective surfaces  $S_A$  and  $S_B$ , and amounts of drug,  $M_A$ ,  $M_B$ . The reservoirs are embedded in the membrane at two different positions,  $x = a$  and  $x = b$ , and they are supposed to be printed in such a way, that they do not screen each other after rolling of the stripe (Figure 6). In frames of the model, which postulates that the thickness of the membrane is much smaller than the planar dimensions of the printed patterns, the releases from the two reservoirs can be considered as independent ones. The resulting kinetics can be obtained then

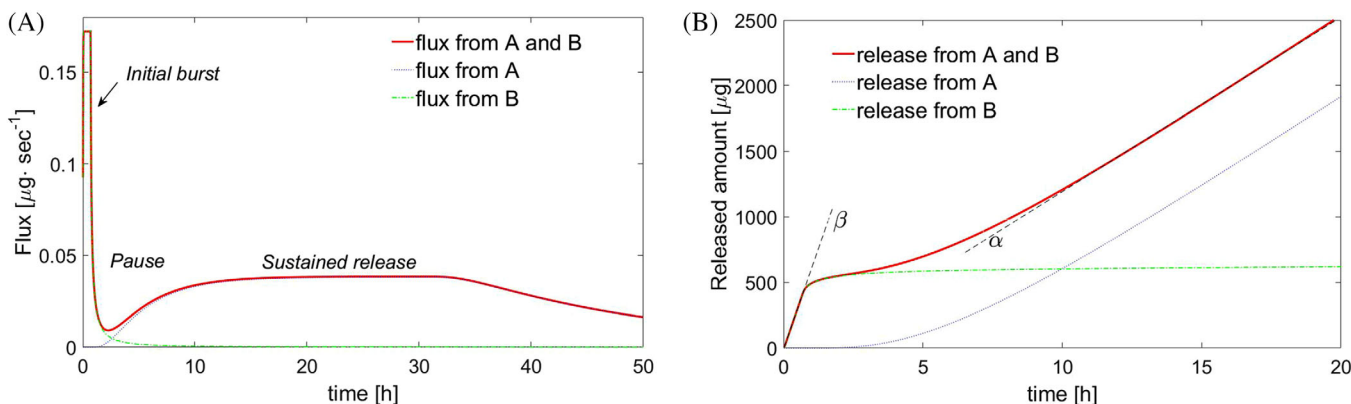
as the superposition of the kinetics two kinetics. Figures 6 and 7 present simulation of the flux and the release kinetics for different variants of the parameters  $S_A$ ,  $M_{ink}^A$ ,  $a$  and  $S_B$ ,  $M_{ink}^B$ ,  $b$ , summarized in the Table 3.

From a therapeutic perspective biphasic release profiles can be used to maintain non constant drug plasmatic concentrations. This plasmatic profile is useful for several therapeutic strategies. For example, Tylenol® 8 Hours is a caplet characterized by an immediate release of acetaminophen providing immediate pain relief, which then is followed by an extended release that grant a long-lasting analgesic effect. These release profile are also important for drugs with extensive first pass metabolism or nonlinear pharmacokinetics, and with chronotherapeutic applications.<sup>[33]</sup>

As illustrated by the Figure 7, it might be possible to find such a configuration of the parameters which provide initial burst, which is almost immediately followed by sustained release phase. Also, it might be possible to program the kinetics with relatively low release rate (pause) after initial burst, before the sustained release phase (Figure 8).

TABLE 3 Simulation parameters for the capsules with 2 independent reservoirs

Simulation	$D \text{ cm}^2 \text{s}^{-1}$	$K$	$C_0, \mu\text{g}\cdot\text{cm}^{-3}$	$h \mu\text{m}$	$S_A \text{ cm}^2$	$M_A \mu\text{g}$	$a \mu\text{m}$	$S_B \text{ cm}^2$	$M_B \mu\text{g}$	$b \mu\text{m}$
1	$1.08 \cdot 10^{-7}$	0.015	$7 \cdot 10^5$	670	0.75	638	133	0.75	319	597
2	-/-	-/-	-/-	1327	4	6380	133	1	638	1261

FIGURE 8 The same as on the Figure 7, *Simulation 2*. The kinetics has two quasi-zero-order phases (marked by the dashed straight lines  $\alpha$  and  $\beta$ ), with a pause between them

#### 4 | CONCLUSION AND OUTLOOK

In summary, we have presented a new approach for the design of drug release devices with adjustable dose and release profiles. The approach is based on the rolling of biocompatible polymer stripes, carrying the drug reservoirs which are formed by ink-jet printing. The position of the reservoir on the stripe is translated into its radial position in the capsule. The release rate can be programmed either by the number of the turns of the stripe around the central water-insoluble stick, or by the position of the drug reservoir on the stripe of a standard length.

As shown by computer simulation, non-trivial kinetics can be programmed by placing several reservoirs, characterized by individual surfaces and amounts of printed drug, at different positions in the membrane. In particular, the kinetics comprising two quasi-zero-order release phases, or kinetics started by the burst release and continued by relatively slow zero-order release can be designed. Obviously, the system may contain a larger number of reservoirs, which can be resolved not only in the axial direction of the capsule, but also in the angular direction. The reservoirs may be partially or fully overlapped after rolling. Also, different reservoirs may contain different drugs, allowing for complex multidrug kinetics.

A number of issues still need to be resolved for the reliable programming of the kinetics. First of all, the factors determined the lag time of the release need to be well understood. The lag time may be determined both by the composition of the ink, but also by the interaction of

the model drug with the polymer matrix. In the present study, we hypothesize that PEG, used as the polymeric glue for the FD crystals, affects the lag time, because of the interference of the polymer swelling with the dissolution kinetics of the fluorescent probe. Although the highly hydrophilic additives complicate the system, they may be interesting also for decoupling the lag time and the release rate, providing more possibilities for the kinetics programming. Swelling and erosion kinetics of the capsules in the release media mimicking the gastro-intestinal tract need to be addressed at the advanced stages of this research.

Computer simulation model was developed for fitting the experimental kinetics. Although it seems to fit well the quasi-zero-order phase of the release, further improvements of the model are necessary to take into account the early and the late stages of the release, and to predict correctly the lag time. Nevertheless, the model may be useful for understanding such phenomena as the retrodiffusion of drug from the reservoir at the intermediate position inside the membrane, and especially for the design of the complex kinetics originating from several drug reservoirs.

The range of potential applications of the rolled-up drug-release system is broad. Sustained and controlled drug delivery systems are already employed for the treatment of several illnesses such as hypertension, rheumatoid arthritis and asthma,<sup>[30,34]</sup> improving significantly the patient compliance and quality of life.<sup>[35]</sup> Besides, delaying the release allows protecting the drug from the stomach environment or vice versa and is necessary for colon-specific delivery important for Crohn's disease and colorectal

cancer treatment.<sup>[36]</sup> Compared to other drug release systems, the one suggested in this paper allows easy modulation of the release rate along with dose of one or more drugs. This provides unique solution for patient suffering of multimorbidity and can ensure bioequivalence between modified release dosage form administered to individuals with different metabolic capacity or clearance rate providing them a tailored solution based on their need.<sup>[2]</sup> Further works will be necessary to choose and optimize the materials considering the application. Improvement should be done over the preparation protocol evaluating other method to stabilize mechanically the roll rather than using adhesives.

## ACKNOWLEDGMENT

The authors gratefully acknowledge financial support by the French National Research Agency, award N° ANR-17-CE18-0021-01. For the assemblage of the rolling machine, special thanks are given to Patrick Lamielle and Cyrille Geney.

## ORCID

Valeriy A. Luchnikov  <https://orcid.org/0000-0003-1740-4899>

## REFERENCES

1. F. Carrasco-Ramiro, R. Peiró-Pastor, B. Aguado, *GeneTher.* **2017**, *24*, 551.
2. J. Brockmöller, M. V. Tzvetkov, *Eur. J. Clin. Pharmacol.* **2008**, *64*, 133.
3. FDA, “Precision Medicine,” can be found under <https://www.fda.gov/medical-devices/vitro-diagnostics/precision-medicine>, **2018**.
4. R. Daly, T. S. Harrington, G. D. Martin, I. M. Hutchings, *Int. J. Pharm.* **2015**, *494*, 554.
5. E. A. Guzzi, M. W. Tibbitt, *Adv. Mater.* **2020**, *32*, 1901994.
6. J. Rantanen, J. Breitkreutz, in *Continuous Manufacturing of Pharmaceuticals* (Ed: P. Kleinebudde), John Wiley & Sons, Ltd, Chichester, UK **2017**, pp. 507–523.
7. N. T. Issa, H. Wathieu, A. Ojo, S. W. Byers, S. Dakshanamurthy, *Curr. Drug Metab.* **2017**, *18*, 556.
8. F. Lévi, A. Okyar, *Expert Opin. Drug Deliv.* **2011**, *8*, 1535.
9. N. Anandabaskar, in *Introduction to Basics of Pharmacology and Toxicology* (Eds: G. Raj, R. Raveendran), Springer, Singapore **2019**. [https://doi.org/10.1007/978-981-32-9779-1\\_16](https://doi.org/10.1007/978-981-32-9779-1_16)
10. K. Wening, J. Breitkreutz, *Int. J. Pharm.* **2011**, *404*, 1.
11. R. Kolakovic, T. Viitala, P. Ihalainen, N. Genina, J. Peltonen, N. Sandler, *Expert Opin Drug Deliv.* **2013**, *10*, 1711.
12. W. Jamróz, J. Szafraniec, M. Kurek, R. Jachowicz, *Pharm. Res.* **2018**, *35*, 176.
13. FDA, “SPRITAM (levetiracetam) Tablets,” can be found under [https://www.accessdata.fda.gov/drugsatfda\\_docs/nda/2015/207958Orig1s000TOC.cfm](https://www.accessdata.fda.gov/drugsatfda_docs/nda/2015/207958Orig1s000TOC.cfm), **2016**.
14. Y. Sun, S. Soh, *Adv. Mater.* **2015**, *27*, 7847.
15. L. K. Prasad, H. Smyth, *Drug Dev. Ind. Pharm.* **2016**, *42*, 1019.
16. K. Liang, D. Brambilla, J.-C. Leroux, *Adv. Mater.* **2019**, *31*, 1805680.
17. N. Sandler, P. Ihalainen, in *Continuous Manufacturing of Pharmaceuticals* (Ed: P. Kleinebudde), John Wiley & Sons, Ltd, Chichester, UK **2017**, pp. 525–549.
18. M. Singh, H. M. Haverinen, P. Dhagat, G. E. Jabbour, *Adv. Mater.* **2010**, *22*, 673.
19. D. Rajjada, N. Genina, D. Fors, E. Wisaeus, J. Peltonen, J. Rantanen, N. Sandler, *J. Pharm. Sci.* **2013**, *102*, 3694.
20. J. Pardeike, D. M. Strohmeier, N. Schrödl, C. Voura, M. Gruber, J. G. Khinast, A. Zimmer, *Int. J. Pharm.* **2011**, *420*, 93.
21. C. Voura, M. M. Gruber, N. Schroedl, D. Strohmeier, B. Eitzinger, W. Bauer, G. Brenn, J. G. Khinast, A. Zimmer, *Pharm. Technol. Eur.* **2011**, *23*, 32.
22. N. Genina, D. Fors, H. Vakili, P. Ihalainen, L. Pohjala, H. Ehlers, I. Kassamakov, E. Haeggström, P. Vuorela, J. Peltonen, N. Sandler, *Eur. J. Pharm. Sci.* **2012**, *47*, 615.
23. V. Y. Prinz, *Microelectron. Eng.* **2003**, *69*, 466.
24. T. Kipp, H. Welsch, Ch. Strelow, Ch. Heyn, D. Heitmann, *Phys. Rev. Lett.* **2006**, *96*, 077403.
25. M. Yu, Y. Huang, J. Ballweg, H. Shin, M. Huang, D. E. Savage, M. G. Lagally, E. W. Dent, R. H. Blick, J. C. Williams, *ACS Nano* **2011**, *5*, 2447.
26. E. J. Smith, W. Xi, D. Makarov, I. Mönch, S. Harazim, V. A. Bolaños Quiñones, C. K. Schmidt, Y. Mei, S. Sanchez, O. G. Schmidt, *Lab Chip* **2012**, *12*, 1917.
27. T. Higuchi, *Drug-Deliv. Device*, **1970**, *13*, 625,214.
28. Mathematical models of drug release, in ‘Strategies to Modify the Drug Release from Pharmaceutical Systems’, Woodhead Publishing **2015**, pp. 63–86.
29. J. Siepmann, R. A. Siegel, F. Siepmann, in *Fundamentals and Applications of Controlled Release Drug Delivery* (Eds: J. Siepmann, R. A. Siegel, M. J. Rathbone, Controlled Release Society), Springer : Controlled Release Society, New York **2012**, <https://doi.org/10.1007/978-1-4614-0881-9>
30. E. Mutschler, H. Knauf, *Clin. Pharmacokinet.* **1999**, *37*, 1.
31. M. Mohammed, J. Syeda, K. Wasan, E. Wasan, *Pharmaceutics* **2017**, *9*, 53.
32. S. Pirillo, V. Pedroni, E. Rueda, M. Luján Ferreira, *Quím.Nova* **2009**, *32*, 1239.
33. *Developing Solid Oral Dosage Forms: Pharmaceutical Theory & Practice* (Eds: Y. Qiu, Y. Chen, G. G. Z. Zhang, L. X. Yu, R. V. Mantri), Elsevier Academic Press, Amsterdam; Boston **2017**.
34. F. E. R. Simons, *Arch Pediatr Adol Med* **1982**, *136*, 790.
35. R. Southwood, V. H. Fleming, G. Huckabee, W. J. Spruill, *Concepts in Clinical Pharmacokinetics*, ASHP, Bethesda, MD **2018**.
36. A. Philip, B. Philip, *OMJ* **2010**, *25*, 70.

## SUPPORTING INFORMATION

Additional supporting information may be found online in the Supporting Information section at the end of the article.

**How to cite this article:** Pedron R, Vandamme T, Luchnikov V. Programming of drug release via rolling-up of patterned biopolymer films. *Nano Select.* **2021**;2:948–957.  
<https://doi.org/10.1002/nano.202000126>